Synthesis and Characterization of Formaldehyde-Bridged Bimetallic Complexes from η^2-Complexes of Molybdenum, Vanadium, and Iron

Dorothy H. Gibson,* Jaime O. Franco, Bradley A. Sleadd, Win Naing, Mark S. Mashuta, and John F. Richardson

Department of Chemistry, University of Louisville, Louisville, Kentucky 40292

Received June 15, 1994®

Reactions of $Cp_2Mo(CH_2O)$ (**1**) and $Cp_2V(CH_2O)$ (**5**) with Lewis acids such as *cis*-$Re(CO)_4(L)(F-BF_3)$ [L = PPh_3 or $P(OPh)_3$] (**2a,b**) or $ZnBr_2$ lead to formaldehyde-bridged complexes **3a**, **3b**, **4**, **6a**, and **6b**; reaction of $Fe(CO)_2[P(OCH_3)_3]_2(CH_2O)$ (**7**) with $ZnBr_2$ yields **8**. All are the μ_2-η^3 type. Two of the products have been characterized by X-ray crystallography. Crystal data for $[Cp_2Mo(CH_2O)]_2ZnBr_2$ (**4**): $C_{22}H_{24}O_2Br_2Mo_2Zn$, space group $P\bar{1}$, a = 14.440(12) Å, b = 15.049(9) Å, c = 12.691(13) Å, α = 104.36(6)°, β = 91.11(8)°, γ = 62.21(5)°, V = 2348(3) Å^3, and Z = 4. The structure was refined to R = 5.2% and R_w = 5.8%. Crystal data for $\{Fe(CO)_2[P(OCH_3)_3]_2(CH_2O)ZnBr_2\}_2$ (**8**): $C_{18}H_{40}Br_4Fe_2O_{18}P_4Zn_2$, space group $P\bar{1}$, a = 10.262(4) Å, b = 11.826(9) Å, c = 10.154(8) Å, α = 95.79(6)°, β = 118.56(5)°, γ = 75.96(5)°, V = 1049(1) Å^3, and Z = 1. The refinement converged with R = 4.1% and R_w = 4.5%. Reaction of Et_4NBr with any of the formaldehyde-bridged complexes readily displaces the Lewis acid and liberates the original formaldehyde complex. In contrast, trifluoroacetic anhydride reacts with **1**, **5**, and **7** with cleavage of the metallaoxirane ring to give (trifluoroacetoxy)methyl trifluoroacetate derivatives **9–11**, respectively.

Introduction

Finding effective methods for the synthesis of oxygenates, particularly C_2 oxygenates such as ethylene glycol, from CO and H_2 (syngas) continues to be of much interest.[1] Although the formation of formaldehyde from syngas is a thermodynamically unfavorable process, the presence of CH_2O in small amounts may lead to critical intermediates needed for the generation of C_2 oxygenates. The pivotal role of metal formaldehyde complexes in Fischer-Tropsch catalytic processes leading to oxygenates has been suggested by several investigators.[2] Furthermore, the possible necessity for bifunctional coordination of formaldehyde has been proposed.[3] To the present time, few formaldehyde-bridged organometallic model compounds have been prepared and little is known about the chemistry of such compounds.[4-6] Particularly few in number are compounds involving late transition metals such as those which are used in catalytic processes.

Three classes of formaldehyde-bridged complexes have been identified in previous work: μ_2-η^2 complexes[4] in which the formaldehyde carbon is bound to one metal and the formaldehyde oxygen is bound to a second metal (zirconium in all of the examples reported); μ_2-η^3 complexes[5] in which the formaldehyde is bound in an η^2-fashion to the first metal and bonded through the oxygen to a second metal (most of these involve Zr as the first, or both, metal centers); one μ_3-η^3 complex[6] in which the formaldehyde carbon is bound to one rhenium center and the oxygen is bridged between two others. Compounds having the last two types of bridging formaldehyde ligands have been structurally characterized; none of the first type has been.

Of the few reactions of formaldehyde complexes which have been examined, those involving strong electrophiles are the most numerous and generally result in metal–oxygen bond cleavage.[7] We report here the results of an investigation of the reactions of a series of η^2-formaldehyde complexes with metal-centered electrophiles which lead to formaldehyde-bridged complexes. Results of reactions between the η^2-formaldehyde complexes and trifluoroacetic anhydride are also described.

Results

1. Reactions of Formaldehyde Complexes with Metal Electrophiles. Recently, we have successfully used the electrophilic nature of rhenium cations bearing

® Abstract published in *Advance ACS Abstracts,* October 1, 1994.

(1) (a) See: Marko, L. *Transition Met. Chem.* **1992,** *17,* 474 (a recent review of work in this area). (b) Izumi, Y.; Chihara, T.; Yamazaki, H.; Iwasawa, Y. *J. Phys. Chem.* **1994,** *98,* 594. (c) Mitchell, W. J.; Wang, Y.; Xie, J.; Weinberg, W. H. *J. Am. Chem. Soc.* **1993,** *115,* 4381.

(2) (a) Keim, W.; Berger, W.; Schlupp, J. *J. Catal.* **1980,** *359.* (b) Feder, H. M.; Rathke, M. *Ann. N.Y. Acad. Sci.* **1980,** *333,* 45. (c) Fahey, D. R. *J. Am. Chem. Soc.* **1981,** *103,* 136. (d) Dombek, B. D. *Adv. Catal.* **1983,** *32,* 325.

(3) (a) Wolczanski, P. T.; Bercaw, J. E. *Acc. Chem. Res.* **1980,** *13,* 121. (b) Keim, W. In *Catalysis in C_1 Chemistry*; Keim, W., Ed.; D. Reidel: Dordrecht, Netherlands, 1983; p 5. (c) Floriani, C. *Pure Appl. Chem.* **1983,** *55,* 1.

(4) μ_2-η^2 complexes: (a) Threlkel, R. S.; Bercaw, J. E. *J. Am. Chem. Soc.* **1981,** *103,* 2650. (b) Barger, P. T.; Bercaw, J. E. *Organometallics* **1984,** *3,* 278. (c) Cutler, A. R.; Chung, T. T. *J. Am. Chem. Soc.* **1986,** *108,* 6069. (d) Cutler, A. R.; Vites, J. C.; Steffey, B. D. *Organometallics* **1991,** *10,* 3432.

(5) μ_2-η^3 complexes: (a) Gambarotta, S.; Floriani, C.; Chiesi-Villa, A.; Guastini, C. *J. Am. Chem. Soc.* **1983,** *105,* 1690. (b) Kropp, K.; Skibbe, V.; Erker, G.; Krüger, C. *J. Am. Chem. Soc.* **1983,** *105,* 3353. (c) Erker, G.; Hoffmann, U.; Zwettler, R.; Betz, P.; Kruger, C. *Angew. Chem., Int. Ed. Engl.* **1989,** *28,* 630. (d) Erker, G.; Mena, M.; Bendix, M. *J. Organomet. Chem.* **1991,** *410,* C5. (e) Curtis, C. J.; Haltiwanger, R. C. *Organometallics* **1991,** *10,* 3220. (f) Berno, P.; Floriani, C.; Chiesi-Villa, A.; Guastini, C. *J. Chem. Soc., Chem. Commun.* **1991,** 109.

(6) μ_3-η^3 complexes: Beringhelli, J.; D'Alfonso, G.; Ciani, G.; Molinari, H. *Organometallics* **1987,** *6,* 194.

(7) Huang, Y.-H.; Gladysz, J. A. *J. Chem. Educ.* **1988,** *65,* 298.

0276-7333/94/2313-4570$04.50/0

weakly coordinated ligands to create CO_2-bridged bimetallic complexes.[8] This strategy has now been applied to the synthesis of formaldehyde-bridged binuclear complexes, as shown in eq 1. A sample of the η^2-

$$\begin{array}{l} Cp_2M(CH_2O) + Re(CO)_4L(F{-}BF_3) \rightarrow \\ \quad \textbf{1}, M = Mo \qquad \textbf{2a}, L = PPh_3 \\ \quad \textbf{5}, M = V \qquad\quad \textbf{2b}, L = P(OPh)_3 \end{array}$$

$$Cp_2M(CH_2O)Re(CO)_4L^+BF_4^- \quad (1)$$

3a, M = Mo; L = PPh_3
3b, M = Mo; L = $P(OPh)_3$
6a, M = V; L = PPh_3
6b, M = V; L = $P(OPh)_3$

formaldehyde complex $Cp_2Mo(CH_2O)$ (**1**) ($Cp = \eta^5$-C_5H_5) was prepared by the method of Herberich et al.;[9] its spectral properties were in agreement with those reported previously.[9,10] Also, DRIFTS (diffuse reflectance infrared Fourier transform spectroscopy) data show ν_{CH} bands at 2907 and 2824 cm^{-1} for the coordinated formaldehyde; these values are closely related to those reported[11] for gaseous formaldehyde at 2843 and 2766 cm^{-1}. Reaction of **1** with *cis*-$Re(CO)_4(PPh_3)(F{-}BF_3)$ (**2a**)[8,12] was conducted in CH_2Cl_2 at −30 °C. The reaction was complete after a few minutes, and after concentration of the solution and the addition of cold ether, a gray solid precipitated from the mixture. Elemental analysis and spectral data are consistent with its formulation as the 1:1 complex $Cp_2Mo(CH_2O)Re(CO)_4(PPh_3)^+BF_4^-$ (**3a**). IR ν_{CO} bands at 2110 (m), 2005 (vs), and 1955 (s) cm^{-1} indicated a cationic complex in which cis geometry at the rhenium center was maintained in **3a**.[8] ^{13}C NMR data showed three low-field doublets (2:1:1 relative intensities) for the carbonyl ligands; the first and third doublets have small J_{PC} values (less than 10 Hz) consistent with cis relationships of the carbonyl and phosphorus ligands while the second doublet has J_{PC} = 55.3 Hz, indicating a trans relationship of phosphorus and one carbonyl. This pattern, also, indicated that cis geometry was maintained at the rhenium atom in **3a**.[13] The carbon spectral data show the formaldehyde carbon at δ 50.78, shifted downfield more than 6 ppm relative to **1**. ^1H NMR data showed the formaldehyde protons at δ 3.00; this resonance is essentially unchanged from **1**. Reaction of **3a** with Et_4NBr liberated **1** in 77% yield and afforded *cis*-$Re(CO)_4(PPh_3)Br$[14] in 84% yield (and, presumably, Et_4NBF_4).

Reaction of **1** with *cis*-$Re(CO)_4[P(OPh)_3](F{-}BF_3)$ (**2b**)[8] was conducted in toluene at −60 °C; the product, **3b**, precipitated from the reaction mixture, as it was formed, as a dark gray solid. Elemental analysis and spectral data indicated a cationic product incorporating the elements of **1** and **2b**, again in a 1:1 manner. Also,

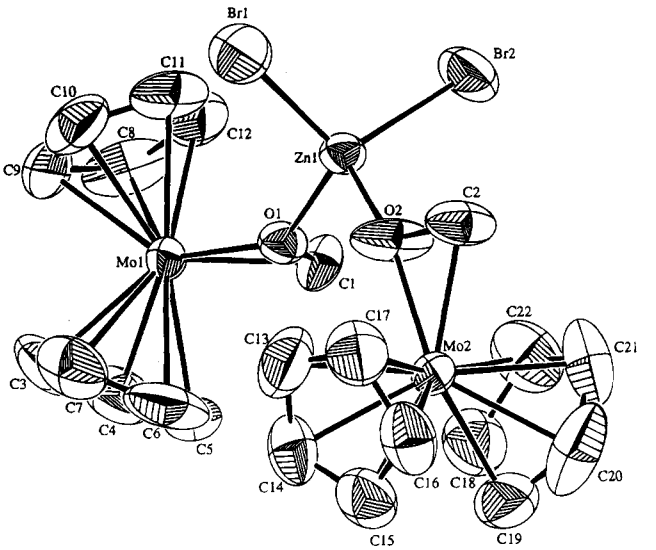

Figure 1. ORTEP drawing of **4** with thermal ellipsoids shown at the 50% probability level.

spectral data were consistent with retention of cis geometry at the rhenium center. NMR spectra of **3b** showed that the formaldehyde carbon resonance had been shifted downfield by about 1 ppm (to δ 45.31) relative to **1** but the formaldehyde protons were nearly unchanged (at δ 2.94). Reaction of **3b** with Et_4NBr regenerated **1** and gave the known *cis*-$Re(CO)_4[P(OPh)_3]Br$.[15]

Reaction of **1** with $ZnBr_2$ in THF afforded a red crystalline product which was characterized by elemental analysis, spectral data, and X-ray crystallography. The results clearly show that two molecules of **1** combined with the $ZnBr_2$ (see Figure 1) to give $[Cp_2Mo(CH_2O)]_2ZnBr_2$ (**4**). The carbon spectrum showed the formaldehyde carbon at δ 40.20, an upfield shift relative to **1**, but the ^1H NMR spectrum showed the formaldehyde protons nearly unchanged at δ 2.96. Efforts to generate a 1:1 adduct between **1** and $ZnBr_2$ resulted in decomposition of **1**. Treatment of **4** with Et_4NBr regenerated **1** in 94% yield.

The procedure for the synthesis of $Cp_2V(CH_2O)$ (**5**) was modified slightly from the original report;[16] higher yields were obtained from reactions conducted for only 20 h (77%) rather than 48 h (53%). Similar to **1**, DRIFTS spectra for **5** showed ν_{CH} bands for the coordinated formaldehyde at 2915 and 2836 cm^{-1}. Reaction of **5** with **2a** was performed in toluene at −10 °C; product precipitation began almost immediately and was completed by chilling the solution to −60 °C. Because of the paramagnetic nature of the vanadium, characterization of the dark green product relied mainly on elemental analysis and IR spectral data. These data were consistent with a compound formulation exactly analogous to that found for molydenum complex **3a** described above, an ionic compound formulated as $Cp_2V(CH_2O)Re(CO)_4(PPh_3)^+BF_4^-$ (**6a**). The IR ν_{CO} bands at 2120 (m), 2010 (vs), and 1960 (s) cm^{-1} again indicated that cis geometry had been maintained at the rhenium center. In the manner of the molybdenum complexes, reaction of **6a** with Et_4NBr liberated **5** and generated *cis*-$Re(CO)_4(PPh_3)Br$.

(8) Gibson, D. H.; Ye, M.; Richardson, J. F. *J. Am. Chem. Soc.* **1992**, *114*, 9716.
(9) Herberich, G.; Okuda, J. *Angew. Chem., Int. Ed. Engl.* **1985**, *24*, 402.
(10) Gambarotta, S.; Floriani, C.; Chiesi-Villa, A.; Guastini, C. *J. Am. Chem. Soc.* **1985**, *107*, 2985.
(11) Alpert, N. L.; Keiser, W. E.; Symanski, H. A. *IR Theory and Practice of Infrared Spectroscopy*; Plenum: New York, 1970; p 158.
(12) See: Beck, W. *Inorg. Synth.* **1990**, *28*, 1 and references cited therein.
(13) Vaughn, G. D.; Strouse, C. E.; Gladysz, J. A. *J. Am. Chem. Soc.* **1986**, *108*, 1462.
(14) McKinney, R. J.; Kaesz, H. D. *J. Am. Chem. Soc.* **1975**, *97*, 3066.
(15) Atwood, J. D.; Brown, T. L. *J. Am. Chem. Soc.* **1976**, *98*, 3155.
(16) Gambarotta, S.; Floriani, C.; Chiesi-Villa, A.; Guastini, C. *J. Am. Chem. Soc.* **1982**, *104*, 2019.

Reaction of **5** with **2b** was conducted at −60 °C in toluene; the dark green product precipitated from the solution as it was formed. The spectral properties of the compound and elemental analysis data were in agreement with its formulation as $Cp_2V(CH_2O)$-$Re(CO)_4[P(OPh)_3]^+BF_4^-$ (**6b**). Also, the IR data showed bands at 2120 (m), 2025 (vs), and 1948 (s) cm^{-1}, indicating that cis geometry at the rhenium center had been maintained. Reaction of **6b** with Et_4NBr liberated **5** and generated *cis*-$Re(CO)_4[P(OPh)_3]Br$.

The synthesis of the complex $Fe(CO)_2[P(OCH_3)_3]_2$-(CH_2O) (**7**) followed the general scheme used by Berke et al.[17] in which formaldehyde displaces dinitrogen from the coordination sphere of the requisite binuclear iron complex, as illustrated in eq 2. However, substantial

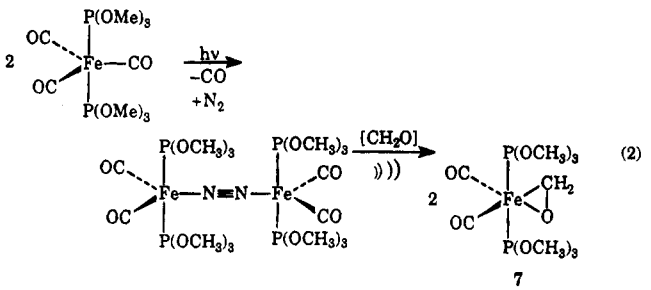

(2)

7

changes were made in the experimental procedures which make them simpler and more efficient. The key to improving the yield of the dinitrogen complex is in the manner of delivery of nitrogen into the vessel in which photolysis of $Fe(CO)_3[P(OCH_3)_3]_2$ is being done; use of a porous diffuser (see Experimental Section), to deliver a stream of very small bubbles, enhances the yield of the dinitrogen complex to 43% (as compared to 19% previously). Reaction of the dinitrogen complex with formaldehyde was conducted by sonicating it in the presence of 37% aqueous formaldehyde solution in a standard ultrasonic cleaning bath for 2 h; the product was purified by crystallization rather than chromatography. The yield of **7** from the dinitrogen complex was increased from 38% to 80% by these modifications.

Efforts to generate bimetallic complexes from reactions of **7** with rhenium complexes **2a** or **2b** were unsuccessful. In both cases it appeared that the decomposition of **7** was catalyzed by the presence of the rhenium complexes since these survive (at least in part) but **7** does not.

Reaction of **7** with excess $ZnBr_2$ yields a yellow crystalline product, **8**, which has been characterized by elemental analysis, spectral properties, and X-ray crystallography. The X-ray data for **8** (see Figure 2) clearly show a 1:1 complex between **7** and the $ZnBr_2$ which exists in the solid state as a dimer. Efforts to generate a 2:1 complex between **7** and $ZnBr_2$ (in the manner described above for **4**) were unsuccessful, probably because of steric crowding around the formaldehyde oxygen atom. ^1H NMR spectral data for **8** show the formaldehyde protons as a triplet at δ 4.10, nearly unchanged from **7**, but the ^{13}C NMR spectrum shows the formaldehyde carbon as a triplet shifted upfield by more than 7 ppm (to δ 65.50) in comparison to **7**. Reaction of **8** with Et_4NBr liberated **7** in 87% yield.

(17) Berke, H.; Bankhardt, W.; Huttner, G.; Seyerl, J. v.; Zsolnai, L. *Chem. Ber.* **1981**, *114*, 2754.

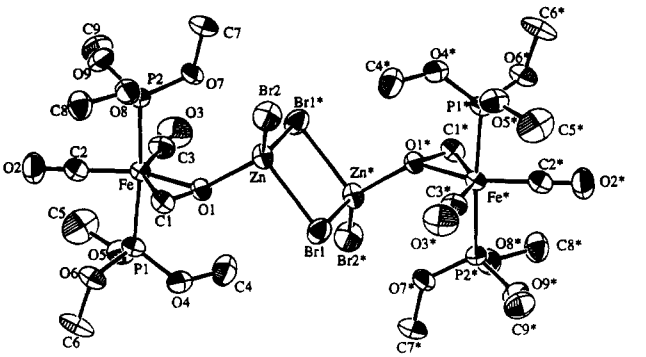

Figure 2. ORTEP drawing of **8** with thermal ellipsoids shown at the 50% probability level.

2. Reactions of Formaldehyde Complexes with $(CF_3CO)_2O$. A series of reactions of the parent formaldehyde complexes, **1**, **5**, and **7**, with trifluoroacetic anhydride (TFAA) have been examined for comparison with the reactions involving metal electrophiles. In each case facile opening of the metallaoxirane ring occurs to give compounds bearing both trifluoroacetoxy and (trifluoroacetoxy)methyl ligands as shown in eq 3; product yields were good, ranging from 65−89%.

$$Cp_2M(CH_2O) + (CF_3CO)_2O \rightarrow$$

1, M = Mo
5, M = V

$$Cp_2M(OCOCF_3)(CH_2OCOCF_3) \quad (3)$$

9, M = Mo
10, M = V

$$Fe(CO)_2[P(OCH_3)_3]_2(CH_2O) + (CF_3CO)_2O \rightarrow$$

7

$$Fe(CO)_2[P(OCH_3)_3]_2(OCOCF_3)(CH_2OCOCF_3)$$

11

Molybdenum complex **1** reacts with TFAA immediately at −35 °C and yields a red solid which has been characterized by elemental analysis as well as by IR, ^1H, and ^{13}C NMR spectral data. All are in agreement with the formulation shown in structure **9**, eq 3. IR spectral data show ν_{CO} bands at 1765 and 1700 cm^{-1}. On the basis of comparisons with related compounds bearing trifluoroacetoxy groups, the higher frequency band is assigned to the ν_{CO} of the (trifluoroacetoxy)-methyl ligand. For example, *trans*-$CpMo(CO)_2[P$-$(OPh)_3]CH_2OCOCF_3$[18] shows ν_{CO} for the ester carbonyl at 1765 cm^{-1} while *cis*-$CpMo(CO)_2[P(OPh)_3](OCOCF_3)$[18] shows ν_{CO} for the trifluoroacetoxy carbonyl at 1698 cm^{-1}. Also, $Os(CO)_2(PPh_3)(CH_2OH)(OCOCF_3)$[19] shows ν_{CO} for the ester carbonyl at 1695 cm^{-1}.

Similarly, vanadium compound **5** afforded a green product after low-temperature reaction with TFAA which gave the elemental analysis results expected for compound **10**, as formulated in eq 3. IR spectral data showed carbonyl stretching bands at 1773 and 1699 cm^{-1}, which are assigned to (trifluoroacetoxy)methyl and trifluoroacetate carbonyls, respectively.

Reaction of formaldehyde complex **7** with TFAA was conducted at room temperature and was complete after

(18) Gibson, D. H.; Franco, J. O.; Richardson, J. F. *Organometallics* **1993**, *12*, 860.
(19) Clark, G. R.; Headford, C. E. L.; Marsden, K.; Roper, W. R. *J. Organomet. Chem.* **1982**, *231*, 335.

1 h. The crude product (**11**) was obtained as an amber oil; yellow crystals were obtained from ether/pentane after chilling the solution to −30 °C. IR spectral data of **11** showed ν_{CO} at 1770 (m) and 1690 (s) cm^{-1}; for the reasons discussed with **9** above, the higher frequency band is assigned to the carbonyl group of the (trifluoroacetoxy)methyl ligand. The ^{13}C NMR data showed inequivalent terminal carbonyl resonances with J_{PC} values which are typical of carbons with cis relationships to phosphorus; ^{31}P NMR data showed a single phosphorus resonance. These data and the elemental analysis were consistent with an octahedral structure for **11**, with the trimethyl phosphite ligands occupying apical positions and the terminal carbonyls cis to one another; this was confirmed by X-ray structural analysis.[20]

Discussion

The ORTEP diagram for one unique molecule of **4** is shown in Figure 1; crystallographic data are summarized in Table 1, atomic positional parameters are shown in Table 2, and selected bond lengths and bond angles are shown in Table 3. The independent molecules show only minor variations in bonding parameters. For simplicity, the discussion will include data for molecule 1 only. Although the formaldehyde ligands are bridged in a μ_2-η^3 fashion, compound **4** is the first such compound to have two η^2-formaldehyde complexes coordinated to a second metal center. In the parent molybdenum complex **1**,[10] the angle between the centroids of the cyclopentadienyl rings is slightly larger than that in the zinc complex **4** (139° rather than 135.13 and 135.55°), presumably because of steric crowding in **4**. The formaldehyde C−O bond lengths are slightly longer in **4** (1.39(2) and 1.38(1) Å as compared to 1.360(3) Å), but the Mo−C bonds involving this ligand are essentially unchanged. The Mo−O bond lengths in **4** are equivalent: Mo1−O1 is 2.066(8) Å and Mo2−O2 is 2.063(9) Å and nearly the same as the Mo−O bond length in **1** (2.056(4) Å). The O−Mo−C bond angles in **4** are increased slightly (38.4(4) and 38.2(4)° as compared to 37.6°); the Mo−O−C angles and the O−C−Mo angles remain nearly the same in **4** as compared to **1**. The Mo1−O1−Zn bond angle is 142.1(4)°, but the Mo2−O2−Zn angle is much larger at 152.9(5)°. At the present time this difference is attributed to crystal packing forces; single resonances for the Cp rings and formaldehyde CH_2 groups are observed in the NMR spectra of **4**.

The ORTEP diagram for **8** is shown in Figure 2; crystallographic data are summarized in Table 1, atomic positional parameters are shown in Table 4, and selected bond lengths and bond angles for this dimer are shown in Table 5. The structure is symmetrical about a crystallographic center of inversion between the zinc atoms. In comparison to the parent compound, **7**,[17] the formaldehyde C−O bond length in zinc complex **8** increases slightly (from 1.32(2) to 1.357(7) Å), the Fe−O bond length contracts slightly (from 2.00(1) to 1.972(4) Å), and the Fe−C bond length remains nearly the same. The O−Fe−C bond angle in **8** is slightly greater than that in **7** (39.7(2)° as compared to 38.2(5)°), the O−C−Fe angle decreases slightly (from 69.7(8) to 68.2(3)°) while the Fe−O−C angle remains the same. Also unchanged in **8**, as compared to **7**, is the coplanar relationship of the metallaoxirane ring to the plane defined by the iron atom and the two terminal CO ligands. The Fe−O−Zn bond angle is 136.8(2)°. Coordination of **1** or **7** to $ZnBr_2$ does not effect any significant changes in bond lengths or bond angles within the original metallaoxirane rings.

Table 1. Summary of Crystallographic Data for $[Cp_2Mo(CH_2O)]_2ZnBr_2$ (4) and $\{Fe(CO)_2[P(OCH_3)_3]_2(CH_2O)ZnBr_2\}_2$ (8)

	4	8
formula	$C_{22}H_{24}Br_2Mo_2O_2Zn$	$C_{18}H_{40}Br_4Fe_2O_{18}P_4Zn_2$
fw	737.50	1230.47
cryst syst	triclinic	triclinic
space group	$P\bar{1}$	$P\bar{1}$
a, Å	14.440(12)	10.262(4)
b, Å	15.049(9)	11.826(9)
c, Å	12.691(13)	10.154(8)
α, deg	104.36(6)	95.79(6)
β, deg	91.11(8)	118.56(5)
γ, deg	62.21(5)	75.96(5)
vol, Å^3	2348(3)	1049(1)
Z	4	1
D_c, g/cm^3	2.09	1.95
cryst dimens, mm	0.49 × 0.18 × 0.10	0.30 × 0.30 × 0.50
cryst descn	red-brown, plate	yellow, block
μ(Mo Kα, cm^{-1})	54.92	58.37
abs corr	DIFABS	DIFABS
trans factors: min/max	0.833/1.214	0.862/1.289
radiation (λ, Å)	Mo Kα (0.710 73)	Mo Kα (0.710 73)
diffractometer	Enraf-Nonius CAD4	CAD4
monochromator	graphite crystal	graphite crystal
temp, °C	22(1)	22(1)
scan range	0.90 + 0.35 tan θ	0.80 + 0.35 tan θ
scan speed, deg min^{-1}	1−5 (in ω)	1−5 (in ω)
max 2θ, deg	50.0	50.0
no. of unique reflns collcd	8223	3673
no. of reflns included ($I_o > 3\sigma(I_o)$)	4906	2889
no. of params	523	218
solution method	direct methods (SIR 88)	Patterson methods (DIRDIF 92 PATTY)
computer hardware	Silicon Graphics Iris Indigo	Silicon Graphics Iris Indigo
computer software	teXsan	teXsan
ext coeff	could not be refined	8.54 × 10^{-7}
agreement factors:[a] R, R_w	0.052, 0.058	0.041, 0.045
function minimized	$\sum w(\|F_o\| - \|F_c\|)^2$	$\sum w(\|F_o\| - \|F_c\|)^2$
GOF	1.93	2.85
largest shift/error	0.01	0.01
weighting scheme	$[\sigma^2(F_o)]^{-1}$	$[\sigma^2(F_o)]^{-1}$
high peak in final diff map	0.92(9)	0.65(9)

[a] $R = \sum||F_o| - |F_c||/\sum|F_o|$; $R_w = [\sum w(|F_o| - |F_c|)^2]/\sum wF_o^2]^{1/2}$.

In addition to **4** and **8**, complexes **3a**, **3b**, **6a**, and **6b** in the present study also appear to be of the μ_2-η^3 type; all are closely related to just one of the previously reported formaldehyde-bridged complexes. Floriani et al.[5f] were able to structurally characterize $[Cp_2Zr(Cl)(CH_2O)Zr(Cl)Cp_2]$; it showed η^2 bonding of the formaldehyde to one Zr atom and bonding through the formaldehyde O atom, only, to the second Zr. Thus the compound was regarded as a Lewis acid adduct of an η^2-formaldehyde complex, although it was not formed in that way. The Zr−O−Zr angle in this compound was 166.9(4)°, much wider than the corresponding angles in **4** and **8**.

(20) $C_{12}H_{22}F_6FeO_{12}P_2$, monoclinic $C2/c$, a = 31.04(2) Å, b = 8.81(1) Å, c = 17.84(2) Å, β = 100.73(7)°; R = 0.106, R_w = 0.119. The molecule was found to have three sites of disorder which were modeled. Two sites involved the rotational orientation of the F atoms about the C of each CF_3 group (two groups of 1/2 occupancy at C5 and three groups of 1/3 occupancy at C7), while the third consists of two overlapping groups of 1/2 occupancy for the C3, O3, C4, and O4 acetoxy unit.

Table 2. Atomic Positional Parameters for 4

atom	*x*	*y*	*z*	B_{eq},[a] Å^2
Mo1	−0.20989(8)	0.26722(9)	0.43572(9)	3.04(3)
Mo2	−0.06089(8)	0.23481(9)	0.87952(9)	3.20(3)
Mo3	−0.28591(8)	−0.25606(9)	−0.20699(9)	3.13(3)
Mo4	−0.44275(8)	−0.23720(8)	0.24505(8)	2.78(2)
Br1	0.0144(1)	0.4061(1)	0.5947(2)	6.64(5)
Br2	0.1765(1)	0.0960(1)	0.5078(2)	6.73(5)
Br3	−0.4859(1)	−0.4253(1)	−0.1606(1)	5.36(4)
Br4	−0.6710(1)	−0.1165(1)	−0.0624(2)	6.15(5)
Zn1	0.0214(1)	0.2485(1)	0.5971(1)	3.37(4)
Zn2	−0.5092(1)	−0.2633(1)	−0.0552(1)	3.31(4)
O1	−0.0984(6)	0.2281(7)	0.5442(6)	3.7(2)
O2	0.0015(8)	0.258(1)	0.7500(7)	7.2(4)
O3	−0.3990(6)	−0.2287(7)	−0.0866(6)	3.6(2)
O4	−0.4979(7)	−0.2665(7)	0.0984(7)	4.5(3)
C1	−0.088(1)	0.134(1)	0.480(1)	4.0(4)
C2	0.073(1)	0.248(1)	0.827(1)	5.5(4)
C3	−0.387(1)	0.343(2)	0.443(2)	7.3(6)
C4	−0.353(2)	0.239(2)	0.426(2)	7.3(6)
C5	−0.308(1)	0.211(2)	0.513(3)	7.8(7)
C6	−0.315(2)	0.295(3)	0.587(2)	8.6(8)
C7	−0.362(1)	0.385(1)	0.547(2)	7.0(5)
C8	−0.180(2)	0.230(2)	0.254(1)	7.0(6)
C9	−0.242(1)	0.339(2)	0.295(2)	8.2(7)
C10	−0.181(2)	0.375(1)	0.357(2)	6.6(5)
C11	−0.086(2)	0.291(2)	0.351(1)	6.7(7)
C12	−0.085(2)	0.208(2)	0.292(2)	7.5(7)
C13	−0.169(2)	0.414(1)	0.907(2)	7.7(6)
C14	−0.230(1)	0.371(1)	0.920(2)	5.8(5)
C15	−0.203(1)	0.329(1)	1.007(1)	6.4(5)
C16	−0.122(1)	0.345(1)	1.050(1)	6.3(5)
C17	−0.100(1)	0.400(1)	0.988(2)	6.7(6)
C18	−0.086(1)	0.096(1)	0.791(2)	7.1(6)
C19	−0.099(2)	0.111(1)	0.904(2)	7.4(6)
C20	−0.003(2)	0.097(2)	0.950(2)	9.3(7)
C21	0.068(1)	0.067(1)	0.860(2)	8.4(6)
C22	0.020(2)	0.069(1)	0.767(2)	7.8(6)
C23	−0.418(1)	−0.134(1)	−0.098(1)	4.0(4)
C24	−0.572(1)	−0.256(1)	0.174(1)	5.7(5)
C25	−0.202(1)	−0.190(2)	−0.076(2)	7.3(5)
C26	−0.194(2)	−0.278(2)	−0.059(2)	7.6(7)
C27	−0.133(1)	−0.363(1)	−0.148(2)	6.0(5)
C28	−0.111(1)	−0.319(2)	−0.223(1)	6.2(5)
C29	−0.154(2)	−0.210(2)	−0.181(2)	6.8(6)
C30	−0.300(2)	−0.235(2)	−0.382(1)	7.8(7)
C31	−0.240(1)	−0.337(2)	−0.387(1)	5.9(5)
C32	−0.302(2)	−0.369(1)	−0.351(1)	6.5(6)
C33	−0.398(1)	−0.290(2)	−0.318(1)	5.1(5)
C34	−0.403(2)	−0.204(1)	−0.334(1)	6.8(5)
C35	−0.277(1)	−0.378(1)	0.215(2)	5.7(5)
C36	−0.348(1)	−0.416(1)	0.189(1)	5.8(4)
C37	−0.410(1)	−0.390(1)	0.286(2)	5.9(5)
C38	−0.381(1)	−0.339(1)	0.366(1)	6.1(5)
C39	−0.300(1)	−0.327(1)	0.326(2)	6.1(5)
C40	−0.520(2)	−0.074(1)	0.212(2)	6.7(6)
C41	−0.418(1)	−0.102(1)	0.232(2)	5.9(5)
C42	−0.413(2)	−0.108(1)	0.342(2)	8.6(7)
C43	−0.516(2)	−0.086(2)	0.380(2)	8.4(6)
C44	−0.577(1)	−0.066(1)	0.302(2)	7.3(6)

[a] $B_{eq} = {}^8/_3\pi^2(U_{11}(aa^*)^2 + U_{22}(bb^*)^2 + U_{33}(cc^*)^2 + 2U_{12}aa^*bb^* \cos\gamma + 2U_{13}aa^*cc^* \cos\beta + 2U_{23}bb^*cc^* \cos\alpha)$.

Formaldehyde complexes **1** and **5** have strongly electron-donating ligands which appear to be needed to bind the formaldehyde carbon strongly; compound **7** has both electron-donating and electron-withdrawing ligands and is less stable toward dissociation of the formaldehyde ligand. By comparison, the bimetallic complexes are reasonably stable in solution, although the rhenium complexes (**3a,b** and **6a,b**) do dissociate to the two starting materials upon standing in polar solvents. The rhenium complexes are more air-sensitive than the zinc complexes, particularly in solution.

The ease with which Et_4NBr displaces the metal center which is bound only through oxygen of the formaldehyde ligand in the bimetallic complexes indicates that the bonding of oxygen to this center is much weaker than to the metal which binds both C and O atoms. The behavior of these η^2-formaldehyde complexes toward metal electrophiles is in sharp contrast to their reactions with carbon electrophiles; the latter reagents (including trifluoroacetic anhydride, as indicated above) will easily break the metallaoxirane ring

Table 3. Selected Bond Lengths (Å) and Bond Angles (deg) for 4

molecule 1		molecule 2	
Bond Lengths			
Mo1−C1	2.16(1)	Mo3−C23	2.12(1)
Mo1−O1	2.066(8)	Mo3−O3	2.080(8)
O1−C1	1.38(1)	O3−C23	1.37(1)
O1−Zn1	1.970(8)	O3−Zn2	1.967(8)
Mo2−C2	2.17(1)	Mo4−C24	2.16(1)
Mo2−O2	2.063(9)	Mo−O4	2.039(8)
O2−C2	1.39(2)	O4−C24	1.37(1)
O2−Zn1	1.929(9)	O4−Zn2	1.963(8)
Br1−Zn1	2.334(3)	Br3−Zn2	2.340(3)
Br2−Zn1	2.362(2)	Br4−Zn2	2.372(2)
Bond Angles			
Mo1−O1−C1	74.5(6)	Mo3−O3−C23	72.4(6)
Mo1−C1−O1	67.3(6)	Mo3−C23−O3	69.5(6)
O1−Mo1−C1	38.2(4)	O3−Mo3−C23	38.1(4)
Mo2−O2−C2	75.0(7)	Mo4−O4−C24	75.8(7)
Mo2−C2−O2	66.6(6)	Mo4−C24−O4	66.2(6)
O2−Mo2−C2	38.4(4)	O4−Mo4−C24	38.0(4)
O1−Zn1−O2	100.4(3)	O3−Zn2−O4	102.7(3)
Mo1−O1−Zn1	142.1(4)	Mo3−O3−Zn2	143.8(4)
Mo2−O2−Zn1	152.9(5)	Mo4−O4−Zn2	151.8(5)
Br1−Zn1−Br2	115.78(9)	Br3−Zn2−Br4	116.00(9)

Table 4. Atomic Positional Parameters for 8

atom	*x*	*y*	*z*	B_{eq}, Å^2
Br1	0.54866(9)	−0.06507(6)	−0.14482(8)	3.83(2)
Br2	0.84935(8)	−0.19058(8)	0.26976(9)	4.59(2)
Zn	0.59182(9)	−0.12269(7)	0.11012(9)	3.19(2)
Fe	0.33125(10)	−0.28150(8)	0.11844(10)	2.51(2)
P1	0.1557(2)	−0.3000(2)	−0.1137(2)	2.78(4)
P2	0.5052(2)	−0.2782(2)	0.3538(2)	3.00(4)
O1	0.4546(4)	−0.2302(4)	0.0451(4)	2.9(1)
O2	0.2542(6)	−0.4738(5)	0.2000(6)	6.0(2)
O3	0.1419(6)	−0.0635(5)	0.1539(6)	5.8(2)
O4	0.1596(5)	−0.2448(4)	−0.2458(5)	3.8(1)
O5	−0.0173(5)	−0.2481(4)	−0.1537(5)	3.9(1)
O6	0.1634(5)	−0.4322(4)	−0.1609(5)	3.7(1)
O7	0.5661(5)	−0.1633(4)	0.3887(5)	3.7(1)
O8	0.6611(5)	−0.3751(4)	0.4143(5)	4.0(1)
O9	0.4627(5)	−0.2958(5)	0.4807(5)	4.2(1)
C1	0.4911(7)	−0.3484(6)	0.0524(7)	3.1(2)
C2	0.2826(8)	−0.3966(7)	0.1663(7)	3.6(2)
C3	0.2148(8)	−0.1474(7)	0.1405(8)	3.5(2)
C4	0.1366(8)	−0.1197(7)	−0.2570(9)	4.8(2)
C5	−0.0798(9)	−0.2760(9)	−0.065(1)	6.3(3)
C6	0.0462(9)	−0.4664(7)	−0.2993(9)	5.5(2)
C7	0.6833(9)	−0.1382(7)	0.5342(8)	5.2(2)
C8	0.6578(8)	−0.4953(7)	0.4159(9)	4.3(2)
C9	0.328(1)	−0.2240(8)	0.4862(9)	5.5(2)

Table 5. Selected Bond Lengths (Å) and Bond Angles (deg) for 8

Bond Lengths			
Fe−C1	2.021(6)	Zn−Br1	2.545(1)
Fe−O1	1.972(4)	Zn−Br1*	2.430(2)
C1−O1	1.357(7)	Zn−Br2	2.322(1)
O1−Zn	1.961(4)		
Bond Angles			
Fe−O1−Zn	136.8(2)	O1−Zn−Br2	119.3(1)
Fe−O1−C1	72.1(3)	Br1*−Zn−Br2	121.86(5)
Fe−C1−O1	68.2(3)	Br1−Zn−Br2	110.79(4)
O1−Fe−C1	39.7(2)	Br1−Zn−Br1*	93.63(4)

by cleaving the M–O bond. The reactions also differ from reactions of one formaldehyde-bridged complex, $[Cp_2Zr(CH_2O)]_2$, with triethylboron[21] which cleaves the metal–formaldehyde carbon bond and removes the methylene unit. In a previous study, reactions of vanadium complex **5** with BF_3 and $TiCl_4$ were reported to result in V–O bond cleavage, but the presumed bimetallic compounds could not be characterized.[16] Efforts are in progress to study further aspects of the chemistry of the formaldehyde-bridged complexes.

Experimental Section

General Data. Reactions and manipulations were carried out under an atmosphere of prepurified nitrogen in Schlenkware or in a Vacuum Atmospheres glovebox (with Dri-train). All glassware was dried in the oven before use. Reagent grade dichloromethane and anhydrous diethyl ether were used as received. Toluene, hexane, and pentane were dried over concentrated sulfuric acid and fractionally distilled before use. THF was dried over KOH and then distilled before use. Solvents used in the glovebox were distilled under nitrogen from the following drying agents: sodium benzophenone ketyl for diethyl ether and tetrahydrofuran (THF); P_2O_5 for dichloromethane, pentane, hexane, and toluene. $Re_2(CO)_{10}$, $MoCl_5$, Cp_2V, and $Fe(CO)_5$ were obtained from Strem Chemical Co. Triphenylphosphine, triphenyl phosphite, formaldehyde (37% in water), benzene-d_6, acetone-d_6, and chloroform-d were obtained from Aldrich. Dichloromethane-d_2 was obtained from Cambridge Isotope Laboratories or Aldrich. The Fine Bubble Discard-a-Stone porous diffuser used in the preparation of **7** was obtained from Lee's Aquarium Products, San Marcos, CA (Catalog No. 12521). $Cp_2Mo(CH_2O)$,[9] *cis*-$Re(CO)_4(PPh_3)(F-BF_3)$,[8] *cis*-$Re(CO)_4[P(OPh)_3](F-BF_3)$,[8] and $Fe(CO)_3[P(OCH_3)]_2$[22] were prepared as described previously. Spectral data were obtained on the following instruments: FT-NMR, Bruker AMX-500; IR, Mattson Galaxy series FT-IR 5000 and Perkin-Elmer 599B. ^1H and ^{13}C NMR chemical shifts were referenced to tetramethylsilane; ^{31}P NMR chemical shifts were referenced to external 85% H_3PO_4. Melting points were obtained on a Thomas-Hoover capillary melting point apparatus and are uncorrected. Elemental analyses were performed by Midwest Microlab, Indianapolis, IN.

Synthesis of $[Cp_2Mo(CH_2O)Re(CO)_4(PPh_3)]^+BF_4^-$ (3a). In a glovebox, $Cp_2Mo(CH_2O)$ (0.14 g, 0.55 mmol) was dissolved in 10 mL of CH_2Cl_2 and the yellow-orange solution was cooled to −30 °C. *cis*-$Re(CO)_4(PPh_3)(FBF_3)$ (0.35 g, 0.54 mmol) was then added in portions. Stirring for 10 min resulted in a dark solution with a purple tinge. The sample was concentrated and slowly diluted with cold ether (30 mL), effecting the precipitation of a gray solid. The mixture was cooled to −65 °C, and the solid was collected by filtration and dried (0.45 g, 92%). It melted with decomposition at 78 °C.

Anal. Calcd for $C_{33}H_{27}BF_4MoO_5PRe$: C, 43.87; H, 3.01. Found: C, 43.64; H, 3.12. IR, ν_{CO} (Nujol mull): 2110 (m), 2005 (vs), 1955 (s) cm^{-1}. DRIFTS (KCl): 2114, 2012, 1956 cm^{-1}. ^1H NMR (CD_2Cl_2, −40 °C): δ 7.60–7.57 and 7.42–7.38 (m, Ph, 15H), 4.92 (s, Cp, 10H), 3.00 (s, CH_2, 2H). ^{13}C NMR (CD_2Cl_2, −40 °C): δ 187.22 (d, CO, J_{PC} = 8.8 Hz), 184.84 (d, CO, J_{PC} = 55.3 Hz), 182.83 (d, CO, J_{PC} = 5.0 Hz) [intensity ratio = 2:1:1], 133.08 (d, J_{PC} = 11.3 Hz), 132.11 (s), 130.02 (d, J_{PC} = 49.1 Hz), 129.37 (d, J_{PC} = 11.3 Hz), 90.65 (s, Cp), 50.78 (s, CH_2). ^{31}P NMR (CD_2Cl_2, −30 °C): δ 13.52 (s).

Reaction of 3a with Et_4NBr. In a glovebox, **3a** (0.05 g, 0.06 mmol) was dissolved in 5 mL of cold (−35 °C) CH_2Cl_2. To the resulting dark solution was added 12 mg (0.06 mmol) of Et_4NBr. The mixture was stirred for 10 min at this temperature and allowed to warm to room temperature, and the solvent was then evaporated to dryness. The yellow-orange residue was taken up in $CDCl_3$, the mixture was filtered through a glass pad into a 5 mm NMR tube, and to it was added known quantities of 1,4-dimethoxybenzene and triphenylphosphine in $CDCl_3$ as internal standards. The ^1H NMR spectral data indicated a 77% yield of $CpMo(CH_2O)$, while the ^{31}P NMR spectral data indicated an 84% yield of *cis*-$Re(CO)_4(PPh_3)Br$.

Synthesis of $Cp_2Mo(CH_2O)Re(CO)_4[P(OPh)_3]^+BF_4^-$ (3b). In a glovebox, $CpMo(CH_2O)$ (0.17 g, 0.66 mmol) was dissolved in 10 mL of toluene and the resulting yellow-orange solution cooled to −60 °C. *cis*-$Re(CO)_4[P(OPh)_3](FBF_3)$ (0.46 g, 0.66 mmol) in 10 mL of cold (−60 °C) toluene was then added. A dark gray solid precipitated instantaneously and was allowed to settle. The supernatant was drawn off, cold hexane (15 mL) was added and the mixture stirred, and then the solid was allowed to settle; this extraction process was repeated twice, and then the product was collected by filtration and dried (0.49 g, 78% yield). It melted with decomposition at 69–70 °C.

Anal. Calcd for $C_{33}H_{27}BF_4MoO_8PRe$: C, 41.67; H, 2.86. Found: C, 42.02; H, 3.28. DRIFTS (KCl), ν_{C-H}: 3119, 2928 cm^{-1}. IR, ν_{CO} (CH_2Cl_2): 2120 (s), 2020 (vs), 1975 (s) cm^{-1}. ^1H NMR (CD_2Cl_2, −20 °C): δ 7.30 (m, Ph, 15H), 5.07 (s, Cp, 10H), 2.94 (s, CH, 2H). ^{13}C NMR (CD_2Cl_2, −20 °C): δ 184.40 (d, CO, J_{PC} = 13.8 Hz), 183.70 (d, CO, J_{PC} = 96.8 Hz), 180.83 (d, CO, J_{PC} = 10.1 Hz) [intensity ratio = 2:1:1], 149.97 (d, J_{PC} = 10.1 Hz), 130.84 (s), 126.94 (s), 120.66 (d, J_{PC} = 5.0 Hz), 90.90 (s, Cp), 45.31 (s, CH_2). ^{31}P NMR (CD_2Cl_2, −20 °C): δ 104.70 (s).

Reaction of 3b with Et_4NBr. In a glovebox, **3b** (0.03 g, 0.03 mmol) was dissolved in 5 mL of cold CH_2Cl_2 (−40 °C); Et_4NBr (0.01 g, 0.05 mmol) was then added, and the mixture was stirred for 10 min. After the solution was warmed to room temperature, the solvent was evaporated to dryness. The residue was taken up in $CDCl_3$ and the mixture filtered through a glass fiber pad into a 5 mm NMR tube. ^1H and ^{31}P NMR spectral data showed only the presence of $Cp_2Mo(CH_2O)$ and *cis*-$Re(CO)_4[P(OPh)_3]Br$.

Synthesis of $[Cp_2Mo(CH_2O)]_2ZnBr_2$ (4). In a glovebox, $Cp_2Mo(CH_2O)$ (0.15 g, 0.59 mmol) was added to 10 mL of THF and the mixture was filtered into a Schlenk flask through a glass pad. $ZnBr_2$ (0.07 g, 0.31 mmol) was then added and the mixture shaken. The resulting red solution was allowed to stand until solid had formed (about 1 h) and was then concentrated to 2 mL; hexane (2 mL) was then added slowly. The red crystalline solid was collected by filtration and dried to give 0.16 g (72% yield) of **4** which decomposed without melting at 123 °C.

Anal. Calcd for $C_{22}H_{24}Br_2Mo_2O_2Zn$: C, 35.83; H, 3.28. Found: C, 35.58; H, 3.32. ^1H NMR (CD_2Cl_2): δ 4.99 (s, Cp), 2.96 (s, CH_2). ^{13}C NMR (CD_2Cl_2): δ 89.56 (s, Cp), 40.20 (s, CH_2).

Reaction of 4 with Et_4NBr. In a glovebox, Et_4NBr (0.01 g, 0.048 mmol) was dissolved in about 0.5 mL of $CDCl_3$ in a small test tube. The solution was transferred by pipet into another test tube containing **4** (9 mg, 0.012 mmol). The mixture was then filtered into a 5 mm NMR tube. To the filtrate was added a known concentration of 1,4-dimethoxybenzene in $CDCl_3$ as the internal standard; the ^1H NMR spectrum indicated a 94% yield of $Cp_2Mo(CH_2O)$.

Synthesis of $Cp_2V(CH_2O)$ (5). In a glovebox, Cp_2V (1.00 g, 5.50 mmol) was dissolved in toluene and to the purple solution was added powdered paraformaldehyde (1.00 g, 33.30 mmol based on the monomer). After 20 h, when the mixture had turned deep green, it was filtered and the filtrate was concentrated under vacuum to 10 mL. The solution was cooled to −30 °C for 2 h and then at −70 °C for 3 h; the resulting deep green crystals were collected by filtration and dried under vacuum (0.90 g, 77% yield). DRIFTS (KBr): ν_{C-H} 3103 cm^{-1} (Cp), ν_{C-H} 2914, 2835 cm^{-1} (CH_2O), ν_{C-O} 1153 cm^{-1} (CH_2O) (lit.[16] ν_{C-O} 1160 cm^{-1}).

(21) Erker, G.; Schmuck, S.; Hoffmann, U. *J. Am. Chem. Soc.* **1991**, *113*, 2330.
(22) Pribula, C. D.; Brown, T. L.; Münck, E. *J. Am. Chem. Soc.* **1974**, *96*, 4149.

Synthesis of $[Cp_2V(CH_2O)Re(CO)_4(PPh_3)]^+BF_4^-$ (6a). In a glovebox, *cis*-$Re(CO)_4(PPh)_3(FBF_3)$ (0.31 g, 0.48 mmol) was stirred in toluene (20 mL) and the mixture cooled to −10 °C. To this was added a cold toluene solution of $Cp_2V(CH_2O)$ (0.10 g, 0.51 mmol), and almost immediately, solid formed. Stirring was discontinued and the mixture cooled to −60 °C. After 45 min, the supernatant was decanted, cold toluene (5 mL) was added, and the mixture was stirred and then allowed to settle; this process was repeated twice. Cold hexane (10 mL) was then added, and the dark-green solid was collected by filtration and dried (0.35 g, 88% yield). The solid decomposed without melting at 80 °C.

Anal. Calcd for $C_{33}H_{27}BF_4O_5PReV$: C, 46.17; H, 3.17. Found: C, 46.21; H, 3.30. IR ν_{CO} (Nujol mull): 2120 (m), 2010 (vs, br), 1960 (s, br) cm^{-1}.

Reaction of 6a with EtN_4Br. In a glovebox, a 0.03 g sample (0.14 mmol) of EtN_4Br was dissolved in 10 mL of CH_2Cl_2 and to the resulting solution was added solid **6a** (0.10 g, 0.12 mmol). The mixture was stirred for 15 min, and the solvent was then evaporated to dryness. The residue was extracted with toluene (2 × 5 mL), and the combined extracts were filtered through Celite. The filtrate was evaporated to dryness under vacuum, the residue was extracted with hexane (2 × 5 mL), and the combined extracts were filtered through a glass pad. The filtrate was evaporated to dryness; $CDCl_3$ was added to the residue, and the mixture was filtered into a 5 mm NMR tube. PPh_3 was added to the sample as an internal standard; the ^{31}P NMR spectrum indicated a 66% yield of *cis*-$Re(CO)_4(PPh)_3Br$.

Synthesis of$[Cp_2V(CH_2O)Re(CO)_4[P(OPh)_3]^+BF_4^-$ (6b). In a glovebox, $Cp_2V(CH_2O)$ (0.13 g, 0.67 mmol) in 10 mL of toluene was cooled to −60 °C and to it was added a cold toluene solution of *cis*-$Re(CO)_4[P(OPh)_3](FBF_3)$ (0.43 g, 0.62 mmol). Immediately, a dark green solid precipitated and was allowed to settle. The supernatant was drawn off, 15 mL of cold hexane was added, and the mixture was stirred; then the solid was allowed to settle. This procedure was repeated three times. After the solid was allowed to settle the third time, it was collected by filtration and dried under vacuum (0.41 g, 74% yield). It melted, with decomposition, at 84−86 °C.

Anal. Calcd for $C_{33}H_{27}BF_4O_8PReV$: C, 43.72; H, 3.00. Found: C, 43.60; H, 3.01. DRIFTS (KCl), ν_{C-H}: 3124, 2941 cm^{-1}. IR, ν_{CO} (Nujol mull): 2120 (m), 2025 (vs), 1948 (s) cm^{-1}.

Reaction of 6b with Et_4NBr. In a glovebox, **6b** (0.05 g, 0.06 mmol) in 5 mL of cold (−30 °C) CH_2Cl_2 was treated with Et_4NBr (0.01 g, 0.05 mmol). After the mixture was stirred for 10 min, it was then allowed to warm to room temperature and the solvent evaporated to dryness. The residue was triturated with toluene, the toluene extract was filtered, and the filtrate was evaporated to dryness. The residue was again triturated, this time with hexane, and filtered and the filtrate evaporated to dryness. To the residue was added $CDCl_3$, the mixture was filtered, and the filtrate was collected in a 5 mm NMR tube. Spectral data (^1H, ^{13}C, and ^{31}P NMR) showed *cis*-$Re(CO)_4[P(OPh)_3]Br$ as the only product. The DRIFTS spectrum of the hexane-insoluble solid was identical to that obtained for $Cp_2V(CH_2O)$.

Synthesis of $[Fe(CO)_2\{P(OMe)_3\}_2]_2N_2$. $Fe(CO)_3[P(OCH_3)_3]_2$ (12.0 g, 30.91 mmol) was dissolved in 700 mL of ether. The resulting yellow solution was transferred into a photolysis vessel equipped with a quartz immersion well and an Ace-Hanovia 450 W medium pressure mercury vapor lamp. Nitrogen was bubbled vigorously for 15 min into the solution via a porous diffuser prior to photolysis (and throughout the photolysis). The mixture was cooled to −30 °C and this temperature maintained throughout the reaction. The solution turned deep green in color within the first hour; the reaction was continued for another 4 h while the progress of the conversion was monitored by IR spectroscopy. The mixture was transferred into a 1 L round-bottomed flask with a side arm and concentrated under vacuum to about 150 mL. A yellow microcrystalline solid precipitated from the solution and was collected by filtration and dried, giving 4.97 g (43% yield) of the product whose spectral properties were identical to those reported by Berke.[17]

Synthesis of $Fe(CO)_2[P(OMe)_3]_2(CH_2O)$ (7). A 500 mL three-necked flask was charged with 50 mL of 37% aqueous formaldehyde solution and 200 mL of ether, and the mixture was sonicated for 5 min in a standard ultrasonic cleaning bath. $[Fe(CO)_2\{P(OCH_3)_3\}_2]_2N_2$ (4.97 g, 6.64 mmol) was added to the mixture which was then sonicated for 2 h. Additional formaldehyde solution (25 mL) was added three times, at 30 min intervals, to maintain the concentration of the monomeric formaldehyde in the ether layer. The progress of the reaction was followed by IR spectroscopy. After 2 h, the ether layer was separated and the aqueous portion was extracted with (3 × 25 mL) ether. The combined ether extracts were washed with water (3 x 50 mL) to remove the remaining formalin. The ether layer was then dried over $MgSO_4$, the mixture was filtered, and the filtrate was concentrated to about 20 mL on a rotary evaporator. Layering the solution with pentane and cooling it to −30 °C for several hours gave deep yellow crystals which were collected by filtration and vacuum-dried (4.13 g, 80% yield). IR and NMR spectral data for this compound were identical to those reported by Berke;[17] the ^1H NMR spectrum (CD_2Cl_2) showed the methylene protons at δ 4.21 as a triplet, and the ^{13}C NMR spectrum showed the methylene carbon as a triplet at δ 73.15.

Reaction of 7 with *cis*-$Re(CO)_4(PPh_3)(FBF_3)$. In a Schlenk flask, **7** (0.10 g, 0.26 mmol) was dissolved in 20 mL of toluene. *cis*-$Re(CO)_4(PPh_3)(FBF_3)$ (0.17 g, 0.26 mmol) was then added, and the mixture was stirred for 4 h. The solvent was then removed under vacuum, and the residue was taken up in CD_2Cl_2. ^1H and ^{13}C NMR spectra indicated the presence of unreacted $Re(CO)_4(PPh_3)(FBF_3)$ and degradation products of the formaldehyde complex.

Reaction of 7 with *cis*-$Re(CO)_4[P(OPh)_3](FBF_3)$. In a Schlenk flask, **7** (0.10 g, 0.26 mmol) was dissolved in 20 mL of toluene. *cis*-$Re(CO)_4[P(OPh)_3](FBF_3)$ (0.18 g, 0.26 mmol) was then added, and the mixture was stirred for 4 h. The solvent was then removed under vacuum, and the residue was taken up in CD_2Cl_2. ^1H and ^{13}C NMR spectra indicated the presence of unreacted *cis*-$Re(CO)_4[P(OPh)_3](FBF_3)$ and degradation products of the formaldehyde complex.

Synthesis of $\{Fe(CO)_2[P(OMe)_3]_2(CH_2O)(ZnBr_2)\}_2$ (8). In a Schlenk flask, $Fe(CO)_2[P(OMe)_3]_2(CH_2O)$ (0.72 g, 1.18 mmol) was dissolved in 30 mL of ether. Anhydrous zinc bromide (0.50 g, 2.22 mmol) was then added, the mixture was stirred for 3 h and then filtered through a glass pad, and the filtrate was concentrated to about 10 mL under vacuum. Layering with 5 mL of pentane and cooling the sample to −30 °C overnight gave a light yellow crystalline solid which was collected by filtration and vacuum-dried (0.83 g, 73% yield). The product, **8**, melted with decomposition at 85 °C.

Anal. Calcd for $C_{18}H_{40}Br_4Fe_2O_{18}P_4Zn_2$: C, 17.57; H, 3.28. Found: C, 17.94; H, 3.38. IR, ν_{CO} (CH_2Cl_2): 2020 (m), 1960 (s) cm^{-1}. ^1H NMR (CD_2Cl_2, −30 °C): δ 4.10 (t, CH_2, 2H), 3.70 (t, OMe, 18H). ^{13}C NMR (CD_2Cl_2, −30 °C): δ 2.12.40 (t, CO, J_{PC} = 45.9 Hz), 206.60 (t, CO, J_{PC}, 30.2 Hz), 65.50 (t, CH_2, J_{PC} = 13.7 Hz), 53.60 (t, OMe, J_{PC} < 1 Hz). ^{31}P NMR (CD_2Cl_2): δ 160.8 (s).

Reaction of $\{[Fe(CO)_2[P(OMe)_3]_2(CH_2O)]ZnBr_2\}_2$ with Et_4NBr. In a Schlenk flask, Et_4NBr (0.010 g, 0.048 mmol) was dissolved in 3 mL of CH_2Cl_2 and the resulting yellow solution was cooled to −30 °C. $\{[Fe(CO)_2[P(OMe)_3]_2(CH_2O)]$-$ZnBr_2\}$ (0.030 g, 0.024 mmol) was then added, and the mixture was allowed to warm to room temperature while being stirred (15 min). The solvent was then removed under vacuum, and after drying for another hour, the residue was taken up in C_6D_6 and the solution filtered through a glass fiber pad into a 5 mm NMR tube. To the sample was added a known concentration of 1,4-dimethoxybenzene in C_6D_6; the ^1H NMR spectrum indicated an 87% yield of $Fe(CO)_2[P(OMe)_3]_2(CH_2O)$.

Synthesis of $Cp_2Mo(CH_2OCOCF_3)(OCOCF_3)$ (9). In a glovebox, $Cp_2Mo(CH_2O)$ (0.10 g, 0.39 mmol) was dissolved in 20 mL of toluene at room temperature and the resulting yellow-orange solution was cooled to −35 °C. Trifluoroacetic anhydride (55 μL, 0.39 mmol) was then added dropwise via microsyringe, causing an immediate color change to red. Stirring was discontinued and the mixture was cooled to −60 °C allowing the red powdery solid to settle. Cold hexane (15 mL) was then added, and after 15 min, the solid that had formed was collected by filtration and dried (0.16 g, 89%). It melted with decomposition at 79 °C.

Anal. Calcd for $C_{15}H_{12}F_6MoO_4$: C, 38.64; 2.59. Found: C, 38.74; H, 2.57. IR, ν_{CO} (Nujol mull): 1765 (s), 1700 (s) cm^{-1}. ^1H NMR (CD_2Cl_2, −30 °C): δ 5.31 (s, Cp), 5.14 (s, CH_2). ^{13}C NMR (CD_2Cl_2, −30 °C): δ 163.52 (q, OC(O), $^2J_{CF}$ = 36.5 Hz), 157.77 (q, OC(O), $^2J_{CF}$ = 40.2 Hz), 114.80 (q, CF_3, J_{CF} = 285.5 Hz), 114.12 (q, CF_3, J_{CF} = 290.5 Hz), 96.36 (s, Cp), 66.43 (s, CH_2).

Synthesis of $Cp_2V(CH_2OC(O)CF_3)(OC(O)CF_3)$ (10). In a glovebox, $Cp_2V(CH_2O)$ (0.10 g, 0.51 mmol) in 15 mL of cold (−60 °C) toluene was treated with $(CF_3CO)_2O$ (0.08 mL, 0.57 mmol) and the dark-green solution was stirred for 15 min. After warming to room temperature and concentrating to 10 mL, hexane (10 mL) was added. The green solid that precipitated was collected by filtration and dried (0.13 g, 65% yield). It melted with decomposition at 98 °C.

Anal. Calcd for $C_{15}H_{12}F_6O_4V$: C, 42.77; H, 2.87. Found: C, 42.87; H, 2.87. DRIFTS (KCl): ν_{C-H} 3119, 2949 cm^{-1}; ν_{CO} 1773 (s), 1699 (vs) cm^{-1}.

Synthesis of $Fe(CO)_2[P(OCH_3)_3]_2(CH_2OC(O)CF_3)(OC(O)CF_3)$ (11). In a Schlenk flask, $Fe(CO)_2[P(OCH_3)_3]_2(CH_2O)$ (0.75 g, 1.92 mmol) was dissolved in 20 mL of ether. Trifluoroacetic anhydride, $(CF_3CO)_2O$ (0.30 mL, 2.08 mmol), was then added, and the mixture was stirred for 1 h. The sample was then evaporated to dryness, leaving an amber-colored oil which was dissolved in a small amount of a 1:1 ether/pentane mixture. Layering with pentane and cooling for 2 days at −30 °C yielded yellow crystals which were collected by filtration and vacuum-dried (0.78 g, 68% yield). The solid melted with decomposition at 43−44 °C.

Anal. Calcd for $C_{13}H_{20}F_6FeO_{12}P_2$: C, 26.02; H, 3.36. Found: C, 26.17; H, 3.31. IR, ν_{CO} (CH_2Cl_2): 2060 (s), 1995 (s), 1770 (m), 1690 (s) cm^{-1}. ^1H NMR (C_6D_6): δ 5.99 (t, CH_2, 2H), 3.27 (t, OCH_3, 18H). ^{13}C NMR (C_6D_6): δ 210.80 (t, CO, J_{PC} = 38.8 Hz), 204.55 (t, CO, J_{PC} = 38.8 Hz), 163.55 (q, CO, J_{FC} = 36.5 Hz), 158.53 (q, CO, J_{FC} = 40.0 Hz), 73.48 (t, CH_2, J_{PC} = 28.9 Hz), 53.24 (t, OMe, J_{PC} = 34.4 Hz). ^{31}P NMR (C_6D_6): δ 148.60 (s).

X-ray Crystal Structure of 4. A suitable single crystal was grown by treating 0.05 g of **1**, dissolved in 2−3 mL of THF, with $ZnBr_2$ (0.02 g) and then allowing the resulting solution to stand for several hours. During this time, red crystals formed on the side of the reaction flask. Data were collected on an Enraf-Nonius CAD4 diffractometer as outlined in Table 1. Atomic positional parameters are shown in Table 2; selected bond lengths and bond angles are shown in Table 3. Of 8223 unique reflections, 4906 were considered observed ($I > 3\sigma(I)$). The structure was solved using direct methods (SIR88) and refined with anisotropic thermal parameters for all non-hydrogen atoms while the calculated positions and isotropic thermal parameters for the H atoms were kept constant. The temperature factors of the hydrogen atoms were set to 1.2 times the temperature factors of the carbon atoms to which they were bonded. The structure was solved for two independent molecules in the asymmetric unit. A final R index of 0.052 with R_w = 0.058 was obtained for 523 variables. All computations were performed using the teXsan[23] package (Molecular Structure Corp.).

X-ray Crystal Structure of 8. A suitable crystal was grown by dissolving a sample of **8** in the minimum amount of ether, layering the solution with an equal volume of pentane, and then allowing the solution to stand for several hours. Data were collected on an Enraf-Nonius CAD4 diffractometer as outlined in Table 1. Atomic positional parameters are shown in Table 4; selected bond lengths and bond angles are shown in Table 5. Of 3673 unique reflections, 2889 were considered observed ($I > 3\sigma(I)$). The structure was solved using heavy-atom direct methods and refined with anisotropic thermal parameters for all non-hydrogen atoms while the calculated positions and isotropic thermal parameters for the H atoms were kept constant. The temperature factors of the hydrogen atoms were set to 1.2 times the temperature factors of the carbon atoms to which they were bonded. A crystallographic center of symmetry is imposed on the dimer. A final R index of 0.041 with R_w = 0.045 was obtained for 218 variables. All computations were performed using the teXsan[23] package (Molecular Structure Corp.).

Acknowledgment. Support of this work by the National Science Foundation (CHE-9112872) and by the NSF/KY EPSCoR Program (EHR-9108764) is gratefully acknowledged. Support of B.A.S. through a GAANN Fellowship from the U.S. Department of Education is also gratefully acknowledged.

Supplementary Material Available: Tables of data collection and refinement parameters, anisotropic thermal parameters, atomic positional parameters, bond distances, bond angles, and torsional angles for **4** and **8** (25 pages). Ordering information is given on any current masthead page.

OM940461R

(23) teXsan: Single Crystal Structure Analysis Software, Version 1.6. Molecular Structure Corp., The Woodlands, TX 77381, 1993.